



저작자표시-비영리-변경금지 2.0 대한민국

이용자는 아래의 조건을 따르는 경우에 한하여 자유롭게

- 이 저작물을 복제, 배포, 전송, 전시, 공연 및 방송할 수 있습니다.

다음과 같은 조건을 따라야 합니다:



저작자표시. 귀하는 원저작자를 표시하여야 합니다.



비영리. 귀하는 이 저작물을 영리 목적으로 이용할 수 없습니다.



변경금지. 귀하는 이 저작물을 개작, 변형 또는 가공할 수 없습니다.

- 귀하는, 이 저작물의 재이용이나 배포의 경우, 이 저작물에 적용된 이용허락조건을 명확하게 나타내어야 합니다.
- 저작권자로부터 별도의 허가를 받으면 이러한 조건들은 적용되지 않습니다.

저작권법에 따른 이용자의 권리는 위의 내용에 의하여 영향을 받지 않습니다.

이것은 [이용허락규약\(Legal Code\)](#)을 이해하기 쉽게 요약한 것입니다.

[Disclaimer](#)

Thesis for the Degree of Master of Engineering

Uncertainties of SO₂ Vertical Column

Density Retrieval using synthetic

Ground-based Direct Sun Hyper-spectral

UV data.

by

Hyeongwoo Kang

Department of Spatial Information Engineering

The Graduate School

Pukyong National University

August 2019

Uncertainties of SO₂ Vertical Column Density
Retrieval using synthetic Ground-based
Direct sun Hyper-spectral UV data
(지상기반 태양 직달광 모의복사휘도자료를
이용한 초분광 자외선으로부터 이산화황
연직칼럼농도의 불확실성 조사)

Advisor: Prof. Han Lim Lee

by

Hyeongwoo Kang

A thesis submitted in partial fulfillment of the requirements

for the degree of

Master of Engineering

in Department of Spatial Information Engineering,

The Graduate School, Pukyong National University

August 2019

Uncertainties of SO₂ Vertical Column Density
Retrieval using synthetic Ground-based Direct Sun
Hyper-spectral UV data

A dissertation

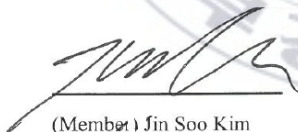
by

Hyeongwoo Kang

Approved by:



(Chairman) Kyung Soo Han



(Member) Jin Soo Kim



(Member) Han Lim Lee

August 2019

List of Contents

1. INTRODUCTION.....	1
2. DATA AND METHOD.....	4
2.1. Principle of DOAS method.....	4
2.2. Ground-based Direct Sun measurement Data	7
3. RESULT.....	15
3.1. Effect of FWHM on SO ₂ VCDs retrieval accuracy.....	15
3.2. Effect of AOD on SO ₂ VCDs retrieval accuracy.....	18
3.3. Effect of SNR on SO ₂ VCDs retrieval accuracy.....	20
3.4. Effect of SZA on SO ₂ VCDs retrieval accuracy.....	22
3.5. Effect of Ozone on SO ₂ VCDs retrieval accuracy.....	24
3.6. Effect of Instrument Condition on SO ₂ VCDs retrieval accuracy.....	26
3.7. Effect of Environment Condition on SO ₂ VCDs retrieval accuracy.....	28
3.8. Uncertainties of SO ₂ VCD in the atmospheric conditions of the Korean Peninsula.....	30
4. CONCLUSION.....	32
5. REFERENCE.....	35

List of Tables

Table 1. Variables used to calculate synthetic radiances	21
--	----

List of Figures

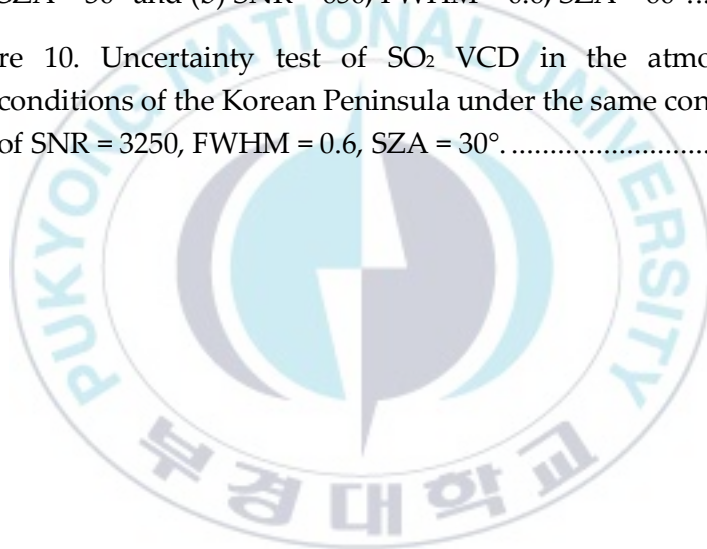
Figure 1. A flowchart of the calculation of ground-based direct sun measurement synthetic radiance.....	7
Figure 2. Example of deconvolution of the DOAS spectrum for evaluating SO ₂ slant column densities. Black line represents the Reference spectrum and red line represents the Measured spectrum.....	15
Figure 3. Uncertainty test of FWHM on SO ₂ vertical column density under the AOD = 0.2, SNR = 650, O ₃ VCD = 300 DU, SZA = 30°.....	22
Figure 4. Uncertainty test of AOD on SO ₂ vertical column density under the FWHM = 0.6, SNR = 650, O ₃ VCD = 300 DU, SZA = 30°.....	25
Figure 5. Uncertainty test of SNR on SO ₂ vertical column density under the FWHM = 0.6, AOD = 0.2, O ₃ VCD = 300 DU, SZA = 30°.....	27
Figure 6. Uncertainty test of SZA on SO ₂ vertical column density under the FWHM = 0.6, AOD = 0.2, O ₃ VCD = 300 DU, SNR = 650.....	29

Figure 7. Uncertainty test of O₃ VCD on SO₂ vertical column density under the FWHM = 0.6, AOD = 0.2, SZA = 30°, SNR = 650.... 31

Figure 8. Uncertainty test of Instrument conditions on SO₂ vertical column density under the (a) AOD = 0.2, O₃ VCD = 300 DU, SZA = 30° and (b) AOD = 0.2, O₃ VCD = 300 DU, SZA = 60°.. 33

Figure 9. Uncertainty test of Environment conditions on SO₂ vertical column density under the (a) SNR = 650, FWHM = 0.6, SZA = 30° and (b) SNR = 650, FWHM = 0.6, SZA = 60° 35

Figure 10. Uncertainty test of SO₂ VCD in the atmosphere conditions of the Korean Peninsula under the same conditions of SNR = 3250, FWHM = 0.6, SZA = 30° 37



지상기반 태양 직달광 모의복사휘도 자료를 이용하여 초분광 자외선센서로부터 이산화황 연직칼럼농도의 불확실성 분석 연구

강 형 우

부경대학교 대학원 공간정보시스템공학과

요약

본 연구에서는 지상관측 기반 태양 직달광 모의복사휘도 생성하고 차등흡수분광법(Differential Optical Absorption Spectroscopy, DOAS)을 이용하여 분광분해능 (Full Width Half Maximum, FWHM), 신호대잡음비 (Signal to Noise Ratio, SNR), 오존 연직칼럼농도 (O_3 Vertical Column Density, O_3 VCD), 에어로졸 광학두께 (Aerosol Optical Depth, AOD), 태양천정각 (Solar Zenith Angle, SZA) 에 대한 지상관측 기반 태양 직달광 장비의 이산화황 연직칼럼농도 (SO_2 Vertical Column Density, SO_2 VCD) 산출 불확실성을 조사하였다. Beer-Lambert Law를 이용하여 직달광 모의복사휘도를 생성하였고 복사전달모델 (Radiative Transfer Model, RTM)인 Vector Linearized Discrete Ordinate Radiative Transfer(VLIDORT)을 이용하여 산란광 모의복사휘도를 생성하였다. 생성된 직달광 모의복사휘도와 산란광 모의복사휘도를 더해줌으로써 최종적인 모의복사휘도를 생성하였다. FWHM = 0.6 nm, AOD = 0.2, O_3 VCD = 300 DU, SZA = 30°의 동일 조건이며 SNR이 650 (3250) 일 때, 모의복사휘도 계산 시 입력값으로 활용된 이산화황 연직칼럼농도와 DOAS 방법을 통해 산출된 이산화황 연직칼럼농도와 비교하여 절대백분위오차 (Absolute Percentage Difference, APD)를 계산한 결과 0.3 DU 농도에서 최대 107% (18%), 1.0 DU 농도에서 최소 30% (11%)로 나타났다. 각 인자 별 이산화황 산출 불확실성 조사 결과 FWHM, SZA, AOD, O_3 VCD의 값이 증가할수록 APD가 증가하였고 그와 반대로 SNR은 값이 증가할수록 APD가 감소하였다. 이에 따라, 본 연구에서는 FWHM, SNR, SZA, O_3 VCD, AOD의 다양한 환경에서 지상 기반 태양 직달광 관측장비가 가지는 이산화황 연직칼럼농도의 산출 불확실성을 정량화하였다.

1. Introduction

Sulfur dioxide (SO₂) which is compounds of sulfur and oxygen forms sulfate aerosols that have an important influence on global atmospheric chemistry and climate. It also directly affects human health such as respiratory disorder and allergen (Hutchinson and Whitby, 1977; Longo et al., 2010; Pope and Dockery, 2006). Active volcanoes are the primary natural source of SO₂, while coal-burning power plants, smelters, and oil refineries are the primary anthropogenic source of SO₂ into the atmosphere (Fioletov et al., 2016). Global Ozone Monitoring Experiment (GOME) equipped on the Earth Research Satellite monitored SO₂ in an artificially generated area of SO₂ such as the Eastern European power plant (Eisinger and Burrows, 1998) and the smelter in Peru and Russia (Khokhar et al., 2008). The past 15 years have seen the launch of three satellite UV instruments capable of detecting near-surface SO₂: the SCanning Imaging Absorption spectroMeter for Atmospheric CHartography (SCIAMACHY), 2002–2012, on board the ENVISAT satellite (Bovensmann et al., 1999); the Global Ozone Monitoring Experiment-2 (GOME 2) instrument, 2006–present, on MetOp-A (Callies et al., 2000); and the Ozone Monitoring

Instrument (OMI) (Levelt et al., 2006), 2004–present, on NASA’s Aura spacecraft (Schoeberl et al., 2006). Many satellites provide SO₂ Vertical Column Density (SO₂ VCD), however strong ozone absorption in the stratosphere and atmospheric scattering above the boundary layer, weakens the UV radiation reaching the surface so that weak absorption features of Planetary Boundary Layer (PBL) SO₂ are difficult to detect by satellite sensor (Knepp et al., 2015; Yan et al., 2017). In addition, satellite-based remote sensing is known to have larger uncertainty than ground-based remote sensing due to many interferences in the atmosphere such as trace gases, aerosol, water vapor, low ambient temperatures in space, and strong cosmic radiation (Lee, 2013). For these reasons, ground-based remote sensing provides more accurate values on the ground and has precise spatial and temporal resolution than satellite-based remote sensing (Li et al., 2000). Ground-based remote sensing helps both in the validation of satellite measurements and the facilitation of a better interpretation of satellite data and their links to surface concentration (Richter et al., 2013). The ground-based multi-axis differential optical absorption spectroscopy (MAX-DOAS) method is used for ground-based SO₂ retrieval. The method is based on scattered sunlight measured in the UV part of the spectrum at different elevation angles with data analyzed using the DOAS

technique (Platt and Stutz, 2008). It was widely used for measurements of SO₂ from the volcano. However, only a few studies have focused on MAX-DOAS measurements of anthropogenic SO₂ (Wang et al., 2014; Wu et al., 2013; Theys et al., 2015). Pandora is another instrument used for SO₂ retrieval. It is a developed instrument for UV and visible spectral measurements, which was primarily designed for direct-sun observations (Fioletov et al., 2016). The ground-based direct sun measurements like Pandora have no errors in air mass factor (AMF) calculations since AMF can be calculated with a simple formula. Prior to calculating the SO₂ VCD using ground-based direct sun measurement, it is necessary to understand and quantify the uncertainties of the various conditions. Therefore, in this study, simulated synthetic radiances were calculated under various conditions, and the uncertainty of the SO₂ VCD from ground-based direct sun measurement was investigated to help validate the SO₂ VCD retrieved from satellites.

2. Data and method

2.1. Principle of DOAS method

In this study, DOAS (Differential Optical Absorption Spectroscopy) method which analyzes the radiance spectrum in the UV, visible, and near-infrared spectral range is used to retrieve SO₂ VCD. The main idea of the DOAS method is to separate the broad-band and narrow-band spectral structures of the absorption spectra that we can calculate the amount of each atmospheric trace gases by reflecting the absorption features of the trace gases (Platt and Stutz, 2008). DOAS method is based on the Beer-Lambert law. The Beer-Lambert law means that intensity of radiance is exponentially reduced by the light path length, the concentration of the trace gases, and the absorption cross-section of the trace gases while passing through the atmosphere. The equation (1) is Beer-Lambert law equation.

$$I(\lambda) = I_0(\lambda)EXP(-LC\sigma) \quad (1)$$

where $I_0(\lambda)$ ($W \text{ nm}^{-1} \text{ cm}^{-2}$) is the intensity of the radiance at the

top of the atmosphere without extinction. The $I(\lambda)$ ($\text{W nm}^{-1} \text{cm}^{-2}$) is the intensity of the radiance at the instrument. As factors affecting the extinction of light, C (molecule cm^{-3}) means the concentration of trace gases exist in the atmosphere, L (cm) means the light path length. The cross-section $\sigma(\lambda, T)$ ($\text{cm}^2 \text{molecule}^{-1}$) which is obtained through lab measurements defines the light absorption at the specific wavelength λ and temperature T (Platt and Stutz, 2008).

Applying DOAS theory to equation (1) leads to equation (2). The principle of DOAS is that the absorption lines are generated by the electron transition of the atoms of the trace gases, and the absorption cross-sections of several trace gases are divided into high-frequency parts and low-frequency parts.

$$I(\lambda) = I_0(\lambda) \text{EXP}(-\sum_{i=0}^n \sigma'_i(\lambda) S_i) \text{EXP}\{-\sum_{i=0}^n \sigma_i(\lambda) S_i + \varepsilon_R(\lambda) + \varepsilon_M(\lambda)\}$$

(2)

In equation (2), $\sigma'_i(\lambda)$ is the part where the absorption curve changes rapidly with wavelength, $\sigma_i(\lambda)$ is the part where the

absorption curve changes slowly with wavelength. $\epsilon_R(\lambda)$ is the Rayleigh scattering and $\epsilon_M(\lambda)$ is the Mie scattering. The intensity of radiance is reduced by Rayleigh scattering, Mie scattering, and trace gases present in the atmosphere, and can be represented by mathematical polynomials with low-frequency part. The Slant Column Density (SCD) of trace gases are retrieved by nonlinear least-squares fitting using the high-frequency characteristics of trace gases except low-frequency parts derived from the aerosols, atmospheric molecules and the slowly changing parts due to the trace gases. By dividing retrieved SCD by AMF, the Vertical Column Density (VCD) is finally calculated.

2.2. Ground-based Direct Sun measurement Data

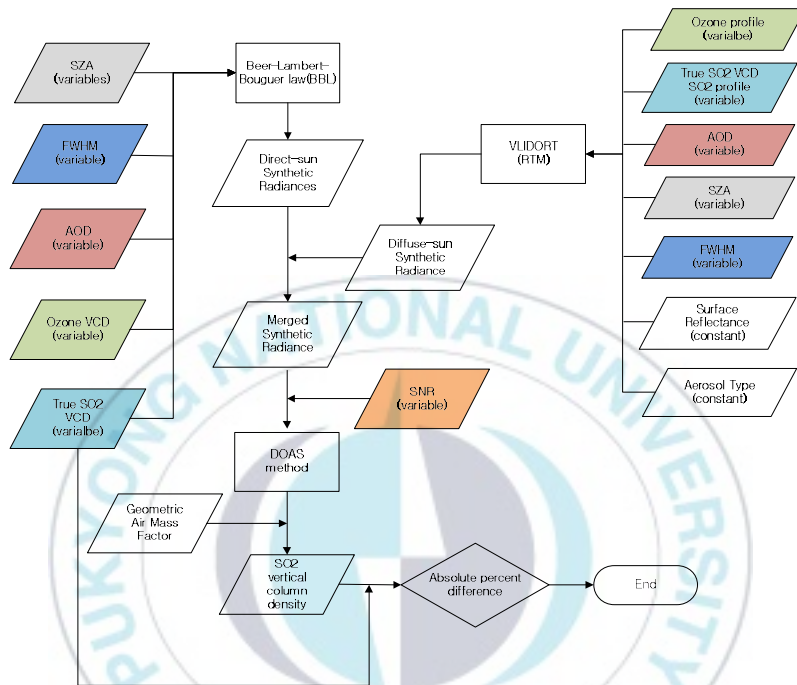


Figure 1. A flowchart of the calculation of ground-based direct sun measurement synthetic radiance.

Figure 1 shows a flowchart of the uncertainty test of SO₂ VCD in ground-based direct sun measurement. In the case of ground-based direct sun measurement, the influence of diffused radiances is negligible because the intensity of the direct radiances is much stronger than that of the diffused radiance in the visible and the near infrared wavelength. However, the effect of diffused radiances

is important in short wavelengths and large SZAs due to strong absorption by O₃ and Rayleigh scattering of atmospheric molecules with wavelength dependence strong enough to cause optical thicknesses above 3.0 at 300 nm wavelength (McKenzie and Johnston, 1995 ; Slusser et al., 2000; Tug and Baumann, 1994). Therefore, in this study, simulated synthetic radiances were calculated by combining synthetic direct radiances calculated from Beer-Lambert equations and synthetic diffused radiances from VLIDORT to investigate the SO₂ VCD uncertainty for the FWHM, SNR, O₃ VCD, AOD, and SZA. The O₃ absorption cross-section of 223K (Bogumil et al., 2003), the 298K sulfur dioxide absorption cross-section (Vandaele et al., 2009), and AOD by wavelength were convoluted with FWHM of 0.2, 0.6, and 1.0 nm condition. In the 360 to 380 nm wavelength range, it is suitable for retrieving SO₂ SCDs since the influence of O₃ is reduced rapidly, however this wavelength range is utilized at the SO₂ SCDs of about 250 DU or more, like the volcanic area, not the low SO₂ SCDs like the city area (Theys et al., 2015). Therefore, the wavelength range for simulated

synthetic radiances is set to 0.2 nm intervals from 290 to 350 nm in this study. FWHM, AOD, O₃ VCDs, SZA, and SO₂ VCD are used as the input variables, and the Beer-Lambert law equation is used to calculate the synthetic direct sun radiance. Simultaneously, the synthetic diffused radiances were calculated using the RTM. In order to calculate synthetic diffused radiance, the same variables that were used to calculate the synthetic direct radiances were used as input data in RTM. In addition, considering the target trace gas is SO₂, aerosol type was fixed with smoke. The aerosol profile is based on the Gaussian distribution function (GDF) described in Jeong et al. (2016) and Hong et al. (2017) and defined as follows:

$$\text{GDF} = \int_{z_{n1}}^{z_{n2}} W \frac{e^{-h(z-z_p)}}{[1+e^{-h(z-z_p)}]^2} dz \quad (3)$$

$$\eta = \frac{\ln(3+\sqrt{8})}{h}, \quad (4)$$

where z_{n1} and z_{n2} are the aerosol lower and upper limits, respectively, W is a normalization constant related to total aerosol loading, h is related to the AHW η , and z_p is the APH (Jeong et

al., 2016; Hong et al., 2017). The simulated synthetic radiances were convolved with a Gaussian slit function with a FWHM of 0.2, 0.6, and 1.0 nm condition to investigate the effect of instrument characteristic. In order to unify the synthetic direct radiances calculated by the Beer-Lambert law and the synthetic diffused radiances calculated by RTM, finally, we calculate the synthetic diffused radiances by multiplying the Solid Angle calculated using Field Of View (FOV) of Pandora, a ground-based direct sun observation instrument currently available in National Aeronautics and Space Administration(NASA). The equation to calculate solid angle is as follows.

$$\Omega = 2\pi(1 - \cos\theta) \quad (5)$$

where Ω is solid angle and θ is FOV/2, The average FOV of Pandora is 2.2°, so θ used in this study is 1.1°. The SNR was randomly applied to synthetic merged radiances which were combined synthetic direct radiances and synthetic diffused radiances. Assuming that the entire variability in Pandora is

instrumental noise, the SNR would be 650:1 (Herman *et al.*, 2015). The SNR values of 920, 1300, and 3250 were selected by co-adding the Pandora SNR in the UV range for 1.5, 2, and 5 times, respectively. The SNRs of 920, 1300, and 3250 were calculated using equation 6 below (Natraj *et al.*, 2011; Park *et al.*, 2018).

$$SNR_i(\lambda) = SNR_a \times \sqrt{\frac{I_i(\lambda)}{I_a}}, \quad (6)$$

where $SNR_i(\lambda)$ and $I_i(\lambda)$ are the i th SNR and radiance at wavelength λ , respectively, I_a is the average value of all synthetic radiances from 290 to 350 nm, and SNR_a is their corresponding SNR. Finally, a total of 3,888 simulated synthetic radiances were calculated in various scenarios. The DOAS fitting wavelength range was set from 311 nm to 329 nm which represents the smallest residual in the range where strong absorption of SO₂. Figure 2 shows an example of deconvolution of DOAS spectra under conditions of SZA = 30 °, SNR = 650, FWHM = 0.6 nm, AOD = 0.2. Next, the retrieved SO₂ SCDs less than 30% for each scenario were divided by AMF to convert to SO₂ VCDs. When using solar

scattering measurement, it is necessary to calculate AMF by using various variables such as profiles of trace gases, aerosol type, and surface reflectance into RTM. Though this study includes diffused radiance, this uncertainty test carried out under the ground-based direct sun measurement, and since AMFs between calculated geometry method and retrieved from RTM are not largely different, therefore, AMF was calculated as simple geometric equation (7).

$$AMF_{direct_sun} = \sec(SZA) \quad (7)$$

The SO₂ SCDs were divided by AMF to calculate the SO₂ VCDs. Finally, The Absolute Percentage Difference (APD) between the two values is calculated by comparing the SO₂ VCDs retrieved by the DOAS method with the true SO₂ VCDs used as the input value to calculate the simulated synthetic radiance. The uncertainty of SO₂ VCDs retrieval for various environmental and instrumental factors was evaluated by comparing the APD of each scenario. Table 1 shows the input values to calculate the synthetic direct radiances and synthetic diffused radiances, respectively.

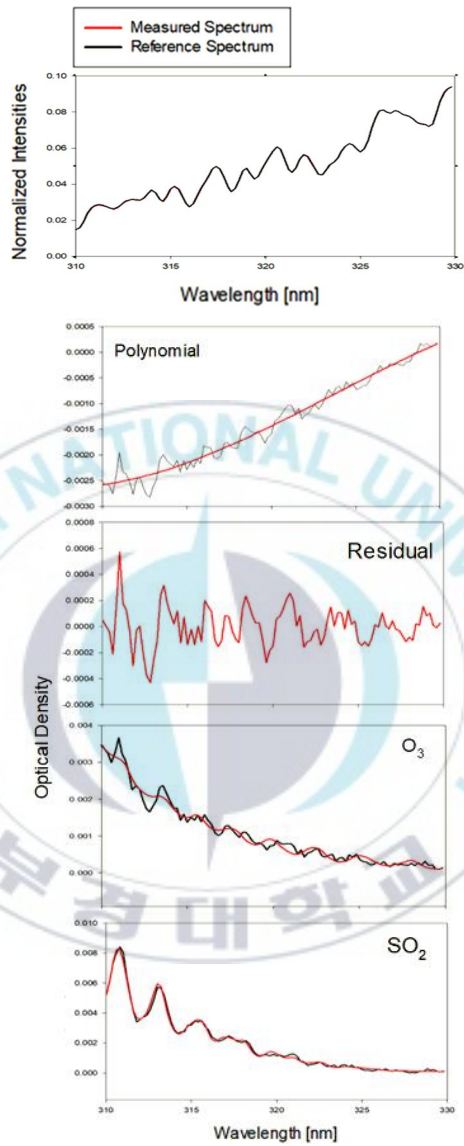


Figure 2. Example of deconvolution of the DOAS spectrum for evaluating SO₂ slant column densities. Black line represents the Reference spectrum and red line represents the Measured spectrum.

Table 1. Variables used to calculate synthetic radiances.

	Variables	Values
Direct radiance	O ₃ VCD	300, 400, and 500 DU
	SZA	30, 40, 50, 60, 70, and 80°
	AOD	0.2, 0.6, 1.0, and 1.5
	SNR	650, 920, 1300, and 3250
	FWHM	0.2, 0.6, and 1.0
	SO ₂ VCD	0.3, 0.4, 0.5, 0.7, 1.0, and 1.5 DU
	O ₃ VCD	300, 400, and 500 DU
	SZA	30, 40, 50, 60, 70, and 80°
	AOD	0.2, 0.6, 1.0, and 1.5
	SNR	650, 920, 1300, and 3250
Diffuse radiance	FWHM	0.2, 0.6, and 1.0
	SO ₂ VCD	0.3, 0.4, 0.5, 0.7, 1.0, and 1.5 DU
	Aerosol Type	Smoke
	Aerosol layer down (upper)	0 (10) km
	Surface Reflectance	0.04
	SO ₂ layer height	0 km

3. Result

3.1. Effect of FWHM on SO₂ VCDs retrieval accuracy

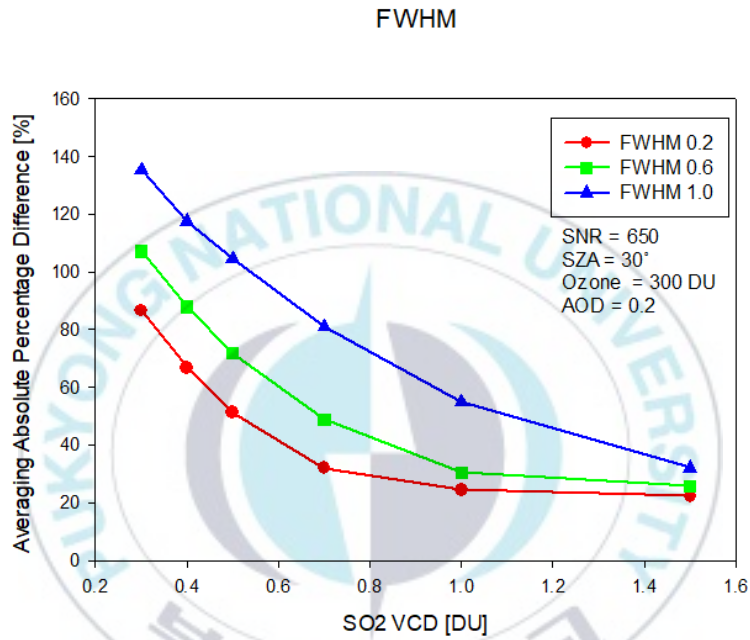


Figure 3. Uncertainty test of FWHM on SO₂ vertical column density under the AOD = 0.2, SNR = 650, O₃ VCD = 300 DU, SZA = 30°.

The FWHM is a slit function, which means the wavelength resolution of the instrument. The better the wavelength resolution,

the better the analysis of the continuous spectroscopic spectrum. Figure 3 shows the results of investigating the uncertainty of the SO₂ VCDs by changing the FWHM to 0.2, 0.6 and 1.0 nm under the same conditions with SNR = 650, O₃ VCD = 300 DU, AOD = 0.2 and SZA = 30°. Figure 3 shows that the smaller the FWHM, the smaller the APD value. The small APD means that the true SO₂ VCDs used as the input value in simulated synthetic radiances calculation are similar to the SO₂ VCDs retrieved using the DOAS method. As the SO₂ VCDs decreased, the difference between true SO₂ VCDs and retrieved SO₂ VCDs was large. In particular, when the SO₂ VCD was 0.3 DU, it showed 85% higher error even at 0.2 nm which is the smallest FWHM in uncertainty test. This means that even if the FWHM of the actual instrument is low when the concentration of SO₂ present in the atmosphere is less than 0.3 DU, it causes a high error of more than 80%. When SO₂ VCD above 1 DU, the SO₂ uncertainties at FWHM 0.2 nm and 0.6 nm were 22 and 25%, respectively, confirming that the SO₂ VCD retrieval for FWHM was not significantly affected. The average difference for FWHM was

about 40%, and it was found that FWHM had a large effect on the SO₂ VCD from 0.5 du to 53%.



3.2. Effect of AOD on SO₂ VCDs retrieval accuracy

Figure 4 shows the results of investigating the uncertainty of the SO₂ VCD according to AOD by changing the AOD to 0.2, 1.0, 0.6, and 1.5 under the same conditions of SNR = 650, O₃ VCD = 300 DU, FWHM = 0.6 nm and SZA = 30°.

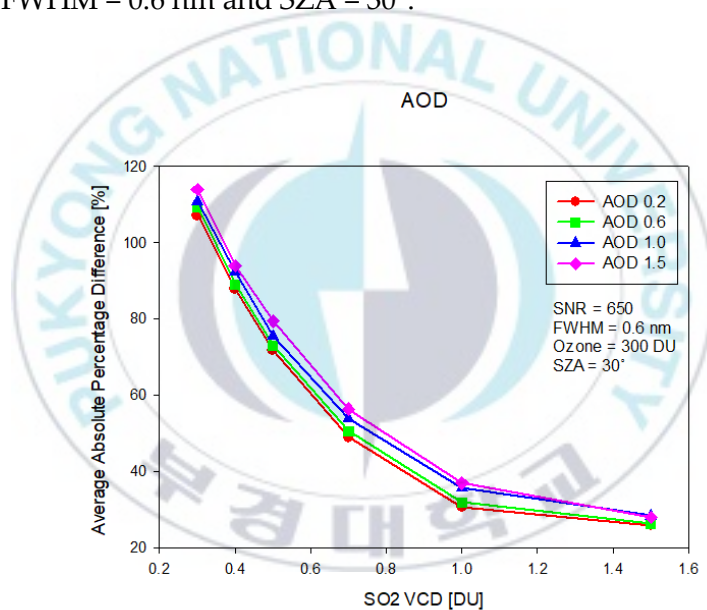


Figure 4. Uncertainty test of AOD on SO₂ vertical column density under the FWHM = 0.6, SNR = 650, O₃ VCD = 300 DU, SZA = 30°.

The small AOD means that the amount of aerosol present in

the atmosphere is relatively small, and the smaller the AOD, the lower the APD between the true SO₂ VCDs and the retrieved SO₂ VCDs. In Fig. 4, the APDs when SO₂ VCD is 0.3 DU showed more than 105% in all four cases of AOD. However, the APD difference according to the AOD was 7% at maximum, which was relatively smaller than FWHM, SNR, and SZA. It means that the SO₂ VCDs uncertainty does not change significantly with a change in AOD. When SO₂ VCD is above 1DU, it converges to 26-28% in all AOD conditions. As previous FWHM converged below 25%, AOD had a greater impact on SO₂ VCD retrieval above 1 DU.

3.3. Effect of SNR on SO₂ VCDs retrieval accuracy

Figure 5 shows that the uncertainty of SO₂ VCDs when SNR is changed to 650, 920, 1300, and 3250 under the same conditions of AOD = 0.2, O₃ VCD = 300 DU, FWHM = 0.6 nm and SZA = 30°.

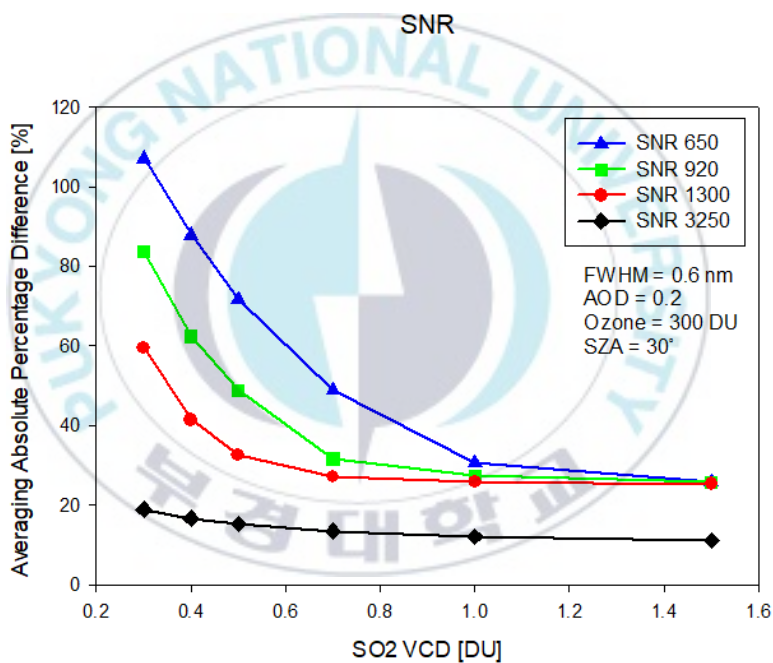


Figure 5. Uncertainty test of SNR on SO₂ vertical column density under the FWHM = 0.6, AOD = 0.2, O₃ VCD = 300 DU, SZA = 30°.

In contrast to previous FWHM, AOD, the larger the value of SNR, the lower the APD. When SO₂ VCD is 0.3 DU, the APDs are 107%, 83%, 59%, and 18% at SNR 650, 920, 1300, and 3250 respectively. The APD was relatively low when compared to the uncertainty of the SO₂ VCDs for the previous FWHM, AOD, but the largest difference occurred for the conditions of SNR in the low SO₂ VCD. This means that the uncertainty of SO₂ VCDs is greatly changed depending on the conditions of SNR when SO₂ concentration present in the atmosphere is below 0.3 DU. When the SO₂ VCD was more than 1.5 DU, SNR converged to 25% at 650, 920, and 1300, but in case of SNR 3250, they showed good performance at less than 12%.

3.4. Effect of SZA on SO₂ VCDs retrieval accuracy

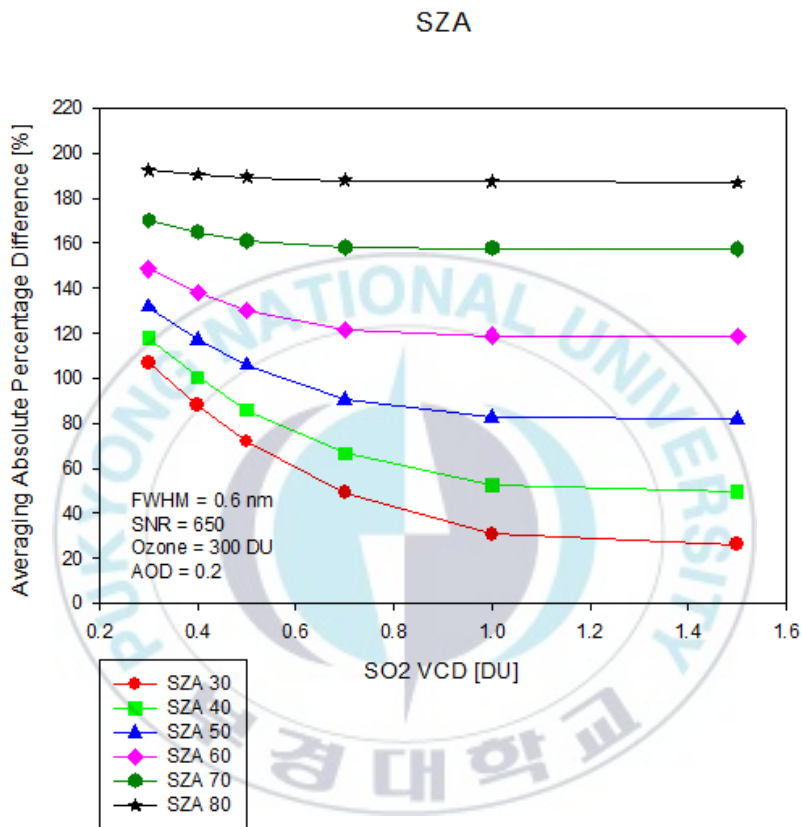


Figure 6. Uncertainty test of SZA on SO₂ vertical column density under the FWHM = 0.6, AOD = 0.2, O₃ VCD = 300 DU, SNR = 650.

Figure 6 shows the result of investigating uncertainty of the

SO₂ VCDs when SZA is changed to 30°, 40°, 50°, 60°, 70°, and 80° under the same conditions of AOD = 0.2, O₃ VCD = 300 DU, FWHM = 0.6 nm, and SNR = 650. SZA is an important factor that determines the light path by the angle between the zenith sky direction and the sun. For large SZA, the light path through the atmosphere increases and therefore Rayleigh scattering, trace gases, aerosol absorption are all increased, leading to reduce sensitivity for SO₂ in the lower troposphere. In the figure 6, the larger the SZA, the higher the APD. This seems to be caused by errors in the calculation of SO₂ VCDs as the light path becomes longer. When the SO₂ VCD of 0.3 DU, a high error of over 105% occurred in all SZA conditions. Above 60 ° SZA, APDs were more than 100% even at the SO₂ VCD was 1 DU. The SO₂ retrieval error caused by SZA has the greatest effect at a maximum of 160%.

3.5. Effect of O₃ on SO₂ VCDs retrieval accuracy

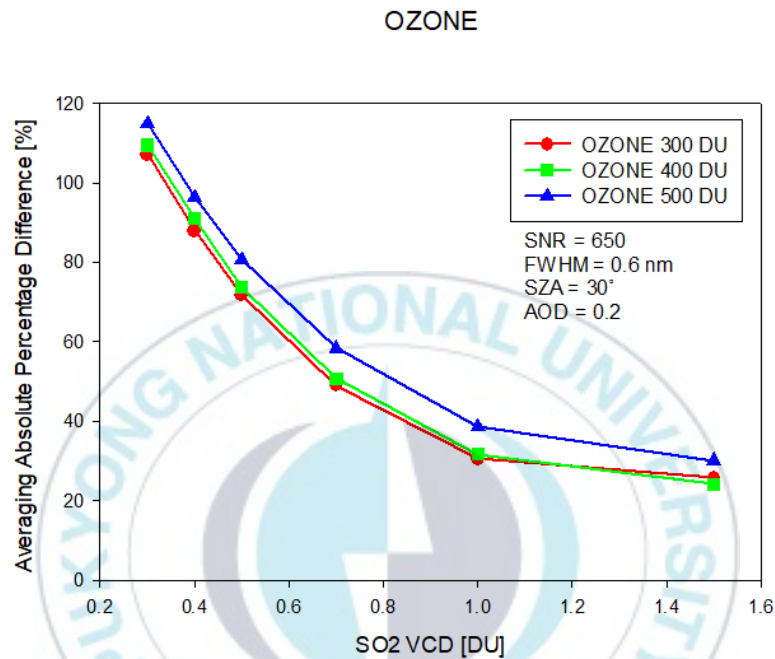


Figure 7. Uncertainty test of O₃ VCD on SO₂ vertical column density under the FWHM = 0.6, AOD = 0.2, SZA = 30°, SNR = 650.

Figure 7 shows the result of SO₂ VCDs retrieval uncertainty by changing the O₃ VCDs to 300, 400, and 500 DU under the same conditions of AOD = 0.2, SZA = 30°, FWHM = 0.6 nm and SNR = 650. The amount of SO₂ is much smaller than that of the total O₃ in

the atmosphere. The weak SO_2 absorption feature by small amounts of PBL SO_2 overlaps with the strong O_3 absorption feature; therefore, we know that uncertainties with the SO_2 SCD retrieval can occur from interferences by the large amount of O_3 in the spectral fitting procedure (Theys et al., 2017; Yan et al., 2017). The higher the O_3 VCD, the higher the APD, which means that the higher the amount of O_3 in the atmosphere, the more error in the retrieval of SO_2 . The APD difference according to the O_3 VCD was 10% at maximum. Among the environmental factors, APD calculated by O_3 VCD was higher than APD from AOD, which means that the O_3 VCD's variation causes higher uncertainty than the AOD's variation.

3.6. Effect of Instrument Condition on SO₂ VCDs retrieval accuracy

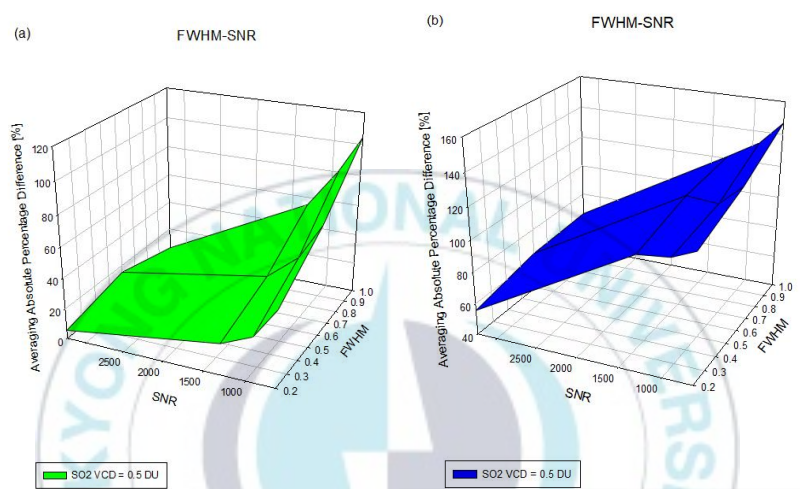


Figure 8. Uncertainty test of Instrument conditions on SO₂ vertical column density under the (a) AOD = 0.2, O₃ VCD = 300 DU, SZA = 30° and (b) AOD = 0.2, O₃ VCD = 300 DU, SZA = 60°.

Figure 8 shows the result of SO₂ VCDs retrieval uncertainty by changing the instrument condition under the same conditions of AOD = 0.2, O₃ VCD = 300 DU. The difference between Figure 8(a) and Figure 8(b) is SZA. Figure 8(a) shows SZA is 30 and Figure 8(b) is SZA 60. Instrument conditions were FWHM and SNR, FWHM

was set to 0.2, 0.6, and 1.0, and SNR was set to 650, 920, 1300, and 3250 to evaluate the uncertainty of SO₂ VCDs retrieval. In both Figures 8(a) and (b), the higher the SNR and the lower the FWHM, the lower the APD value. When the SZA is 30, FWHM is 0.2, and the SNR is 3250 the minimum APD is 5%, the maximum APD is 104%. When the SZA was 60, the minimum APD was 60% and the maximum APD was 147%. Comparing Fig. 8 (a) and (b), it shows a high retrieval error of more than 50% under the same condition of FWHM = 0.2 and SNR = 3250, which means that the effect on SZA is very large.

3.7. Effect of Environment Condition on SO₂ VCDs retrieval accuracy

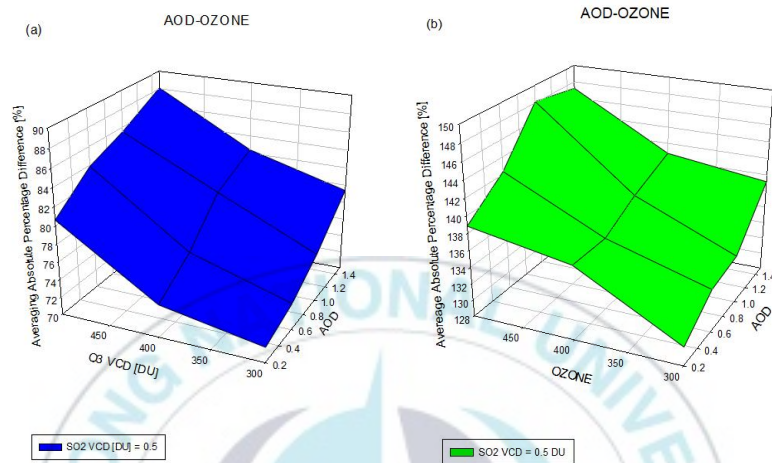


Figure 9. Uncertainty test of Environment conditions on SO₂ vertical column density under the (a) SNR = 650, FWHM = 0.6, SZA = 30° and (b) SNR = 650, FWHM = 0.6, SZA = 60°

Figure 9 shows the result of SO₂ VCDs retrieval uncertainty by changing the environment condition under the same conditions of SNR = 650, FWHM = 0.6 nm. When the SZA is 30, the minimum APD is 71% when the AOD is 0.2 and the O₃ VCD is 300 DU, and when the AOD is 1.5 and the O₃ VCD is 500 DU, the maximum APD is 88%. APDs difference between Figure 9 (a) and (b) shows retrieval error of SO₂ VCD nearly double according to SZA. When

the SZA was 60, the minimum APD was 130% and the maximum APD was 148%. The environmental conditions cause an overall higher SO₂ VCD retrieval error than the instrumental conditions.



3.8. Uncertainties of SO₂ VCD in the atmospheric conditions of the Korean Peninsula

Korean Peninsula environmental condition

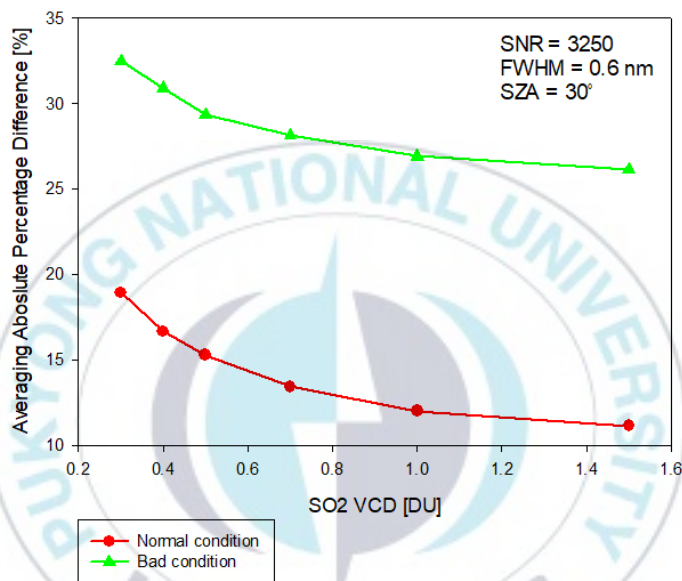
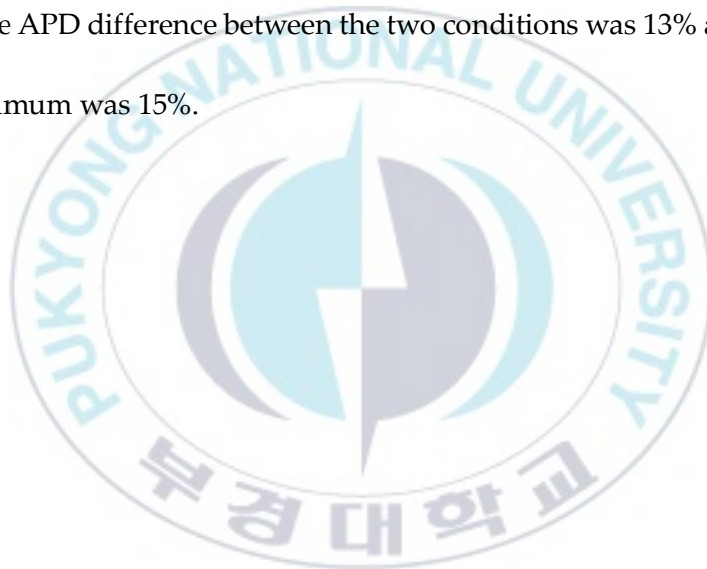


Figure 10. Uncertainty test of SO₂ VCD in the atmosphere conditions of the Korean Peninsula under the same conditions of SNR = 3250, FWHM = 0.6, SZA = 30°

Figure 10 shows the uncertainty of SO₂ VCDs in an air environment similar to Korea Peninsula. According to J. Kim et al (2017), the average concentration of O₃ in the Korean peninsula is 310 DU and the maximum concentration is over 400 DU. The mean

and maximum values of AOD were 0.2 and 1.0 (S. Kim et al., 2007). Normal condition was set to AOD = 0.2, O₃ VCD = 300 DU, and bad condition was set to AOD = 1.0 and O₃ VCD = 400 DU. FWHM, SNR, and SZA all set to the same condition. In bad condition, the SO₂ VCD retrieval error was larger than normal condition. The average of the APD difference between the two conditions was 13% and the maximum was 15%.



4. Conclusion

In this study, we investigated the uncertainty of the SO₂ VCD in ground-based direct sun measurement for FWHM, SNR, O₃ VCD, AOD, and SZA. The simulated synthetic radiances of the ground-based direct sun measurement instrument was produced by adding the synthetic diffused radiances through the RTM to the synthetic direct radiances calculated from the Beer-Lambert law. The SO₂ SCDs were calculated by the DOAS method. The retrieved SO₂ SCDs were divided into AMF calculated by the geometrical measurement structure of the ground-based direct sun measurement to calculate the SO₂ VCDs. The uncertainties of SO₂ VCDs were quantified by comparing true SO₂ VCDs, which was used as input data in simulated synthetic radiance calculation, and retrieved SO₂ VCDs. As a result of comparing the APDs of each factor, it was confirmed that the larger the value of FWHM, AOD, SZA, and O₃ VCD, the greater the difference between the true SO₂ VCDs and retrieved SO₂ VCDs. In contrast, the smaller the SNR,

the larger the difference between the true SO₂ VCDs and retrieved SO₂ VCDs. In uncertainty test of SO₂ VCD for SZA, when the SO₂ VCD was over 1 DU, the APD was 30% at 30° SZA and 118% at 60° SZA. When the SO₂ VCD was more than 1 DU, it showed more than 100% uncertainty in high SZA. This means that SZA had the greatest effect on the retrieval of SO₂ VCD through all the factors. It was confirmed that FWHM, SNR, and SZA had more influence on SO₂ VCD retrieval than AOD and O₃ VCD. When the SO₂ VCD was more than 1.5 DU, SNR converged to 25% at 650, 920, and 1300, but showed good performance at less than 10% at SNR 3250. These results suggest that it is more efficient to increase snr than to reduce FWHM although increasing the SNR has the disadvantage that the time resolution is reduced.

In this study, for the first time, we used ground-based direct sun measurement simulated synthetic radiances to quantify the uncertainty of the SO₂ VCD for various conditions. Based on this study, it is possible to qualitatively and quantitatively evaluate the

uncertainty of SO₂ VCD retrieval errors in ground-based direct sun measurement instrument. Furthermore, in the future, it is possible to suggest the specification of an instrument suitable for each local environment conditions and to validate satellite-based remote sensing more accurately.



5. Reference

- Bogumil, K., J. Orphal, T. Homann, S. Voigt, P. Spietz, O.C. Fleischmann, and J. Frerick, 2003. Measurements of molecular absorption spectra with the SCIAMACHY pre-flight model: instrument characterization and reference data for atmospheric remote-sensing in the 230–2380 nm region, *Journal of Photochemistry and Photobiology A: Chemistry*, 157(2-3): 167-184. [https://doi.org/10.1016/S1010-6030\(03\)00062-5](https://doi.org/10.1016/S1010-6030(03)00062-5)
- Bovensmann, H., J.P. Burrows, M. Buchwitz, J. Frerick, S. Noël, V.V. Rozanov, and A.P.H. Goede, 1999. SCIAMACHY: Mission objectives and measurement modes, *Journal of the atmospheric sciences*, 56(2): 127-150. [https://doi.org/10.1175/1520-0469\(1999\)056<0127:SMOAMM>2.0.CO;2](https://doi.org/10.1175/1520-0469(1999)056<0127:SMOAMM>2.0.CO;2)
- Callies, J., E. Corpaccioli, M. Eisinger, A. Hahne, and A. Lefebvre, 2000. GOME-2-Metop's second-generation sensor for operational ozone monitoring, *ESA bulletin*, 102: 28-36.

Eisinger, M. and J.P. Burrows, 1998. Tropospheric sulfur dioxide observed by the ERS-2 GOME instrument, *Geophysical Research Letters*, 25(22): 4177-4180. <https://doi.org/10.1029/1998GL900128>

Fioletov, V. E., C.A. McLinden, A. Cede, J. Davies, C. Mihele, S. Natcheva, and J. O'Brien, 2016. Sulfur dioxide (SO₂) vertical column density measurements by Pandora spectrometer over the Canadian oil sands, *Atmospheric Measurement Techniques*, 9(7): 2961-2976. <https://doi.org/10.5194/amt-9-2961-2016>

Herman, J., R. Evans, A. Cede, N. Abuhassan, I. Petropavlovskikh, and G. McConville, 2015. Comparison of ozone retrievals from the Pandora spectrometer system and Dobson spectrophotometer in Boulder, Colorado, *Atmospheric Measurement Techniques*, 8(8): 3407-3418. <https://doi.org/10.5194/amt-8-3407-2015>

Hutchinson, T. C. and L.M. Whitby, 1977. The effects of acid rainfall and heavy metal particulates on a boreal forest ecosystem near

the Sudbury smelting region of Canada, *Water, Air, and Soil Pollution*, 7(4): 421-438. <https://doi.org/10.1007/BF0028554>

Khokhar, M. F., U. Platt, and T. Wagner, 2008. Temporal trends of anthropogenic SO₂ emitted by non-ferrous metal smelters in Peru and Russia estimated from satellite observations, *Atmospheric Chemistry and Physics Discussions*, 8(5): 17393-17422. <https://doi.org/10.5194/acpd-8-17393-2008>

Kim, J., Kim, J., Cho, H. K., Herman, J., Park, S. S., Lim, H. K., ... & Lee, Y. G. (2017). Intercomparison of total column ozone data from the Pandora spectrophotometer with Dobson, Brewer, and OMI measurements over Seoul, Korea. *Atmospheric Measurement Techniques*, 10(10), 3661-3676.

Kim, S. W., Yoon, S. C., Kim, J., & Kim, S. Y. (2007). Seasonal and monthly variations of columnar aerosol optical properties over east Asia determined from multi-year MODIS, LIDAR, and AERONET Sun/sky radiometer measurements.

Atmospheric Environment, 41(8), 1634-1651.

Knepp, T., M. Pippin, J. Crawford, G. Chen, J. Szykman, R. Long, and R. Delgado, 2015. Estimating surface NO₂ and SO₂ mixing ratios from fast-response total column observations and potential application to geostationary missions, *Journal of atmospheric chemistry*, 72(3-4): 261-286. <https://doi.org/10.1007/s10874-013-9257-6>

Lee, H., 2013. Comparison of Nitrogen Dioxide Retrieved by MAX-DOAS and OMI measurements in Seoul, *Korean Journal of Remote Sensing*, 29(2): 235-241 (in Korean with English abstract). <https://doi.org/10.7780/kjrs.2013.29.2.7>

Levelt, P. F., G.H. van den Oord, M.R. Dobber, A. Malkki, H. Visser, J. de Vries, and H. Saari, 2006. The ozone monitoring instrument, *IEEE Transactions on geoscience and remote sensing*, 44(5): 1093-1101. <https://doi.org/10.1109/TGRS.2006.872333>

Li, Z., P. Wang, and J. Cihlar, 2000. A simple and efficient method for retrieving surface UV radiation dose rate from

satellite, *Journal of Geophysical Research: Atmospheres*, 105(D4):
5027-5036. <https://doi.org/10.1029/1999JD900124>

Longo, B. M., W. Yang, J.B. Green, F.L. Crosby, and V.L. Crosby,
2010. Acute health effects associated with exposure to volcanic
air pollution (vog) from increased activity at Kilauea Volcano
in 2008, *Journal of Toxicology and Environmental Health*, 73(20):
1370-1381. <https://doi.org/10.1080/15287394.2010.497440>

McKenzie, R. L. and P.V. Johnston, 1995. Comment on “Problems
of UV-B radiation measurements in biological research:
Critical remarks on current techniques and suggestions for
improvements” by H. Tüg and MEM Baumann, *Geophysical
research letters*, 22(9): 1157-1158.
<https://doi.org/10.1029/95GL01115>

Natraj, V., X. Liu, S. Kulawik, K. Chance, R. Chatfield, D.P.
Edwards, and R. Spurr, 2011. Multi-spectral sensitivity studies
for the retrieval of tropospheric and lowermost tropospheric
ozone from simulated clear-sky GEO-CAPE

measurements, *Atmospheric Environment*, 45(39): 7151-7165.

<https://doi.org/10.1016/j.atmosenv.2011.09.014>

Park, J., H. Lee, J. Kim, J. Herman, W. Kim, H. Hong, and D. Kim, 2018. Retrieval Accuracy of HCHO Vertical Column Density from Ground-Based Direct-Sun Measurement and First HCHO Column Measurement Using Pandora, *Remote Sensing*, 10(2): 173. <https://doi.org/10.3390/rs10020173>

Platt, U. and J. Stutz, 2008. *Differential absorption spectroscopy*. In *Differential Optical Absorption Spectroscopy*, Springer, Berlin, Heidelberg. pp. 135-174. https://doi.org/10.1007/978-3-540-75776-4_6

Pope III, C. A. and D.W. Dockery, 2006. Health effects of fine particulate air pollution: lines that connect, *Journal of the air & waste management association*, 56(6): 709-742. <https://doi.org/10.1080/10473289.2006.10464485>

Richter, A., M. Weber, J.P. Burrows, J.C. Lambert, and A. Van Gijsel, 2014. Validation strategy for satellite observations of

tropospheric reactive gases, *Annals of Geophysics*, 56.
doi:10.4401/ag-6335, 2013

Schoeberl, M. R., A.R. Douglass, E. Hilsenrath, P.K. Bhartia, R. Beer,
J.W. Waters, and P.F. Levelt, 2006. Overview of the EOS Aura
mission, *IEEE Transactions on Geoscience and Remote Sensing*,
44(5): 1066-1074. doi: 10.1109/TGRS.2005.861950

Slusser, J., J. Gibson, D. Bigelow, D. Kolinski, P. Disterhoft, K. Lantz,
and A. Beaubien, 2000. Langley method of calibrating UV
filter radiometers, *Journal of Geophysical Research: Atmospheres*,
105(D4): 4841-4849. <https://doi.org/10.1029/1999JD900451>

Theys, N., De Smedt, I., Van Gent, J., Danckaert, T., Wang, T.,
Hendrick, F., ... & Krotkov, N. (2015). Sulfur dioxide vertical
column DOAS retrievals from the Ozone Monitoring
Instrument: Global observations and comparison to ground-
based and satellite data. *Journal of Geophysical Research:
Atmospheres*, 120(6), 2470-2491.

Theys, N., Smedt, I. D., Yu, H., Danckaert, T., Gent, J. V., Hörmann,

C., ... & Pedergnana, M. (2017). Sulfur dioxide retrievals from TROPOMI onboard Sentinel-5 Precursor: algorithm theoretical basis. *Atmospheric Measurement Techniques*, 10(1).

Tüg, H. and M.E. Baumann, 1994. Problems of UV-B radiation measurements in biological research. Critical remarks on current techniques and suggestions for improvements, *Geophysical research letters*, 21(8): 689-692.
<https://doi.org/10.1029/94GL00373>

Vandaele, A. C., C. Hermans, and S. Fally, 2009. Fourier transform measurements of SO₂ absorption cross sections: II.: Temperature dependence in the 29 000–44 000 cm⁻¹ (227–345 nm) region, *Journal of Quantitative Spectroscopy and Radiative Transfer*, 110(18): 2115-2126.
<https://doi.org/10.1016/j.jqsrt.2009.05.006>

Wang, T., F. Hendrick, P. Wang, G. Tang, K. Clémer, H. Yu, and G. Pinardi, 2014. Evaluation of tropospheric SO₂ retrieved from MAX-DOAS measurements in Xianghe, China, *Atmospheric*

Chemistry and Physics, 14(20): 11149-11164.

<https://doi.org/10.5194/acp-14-11149-2014>

Wu, F. C., P.H. Xie, A. Li, K.L. Chan, A. Hartl, Y. Wang, and J.G. Liu,

2013. Observations of SO₂ and NO₂ by mobile DOAS in the

Guangzhou eastern area during the Asian Games 2010,

Atmospheric Measurement Techniques, 6(9): 2277-2292.

<https://doi.org/10.5194/amt-6-2277-2013>

Yan, H., X. Li, W. Wang, X. Zhang, L. Chen, D. Han, and L. Gao.

2017. Comparison of SO₂ column retrievals from BRD and

DOAS algorithms, *Science China Earth Sciences*, 60(9): 1694-

1706. <https://doi.org/10.1007/s11430-016-9057-6>